Atmos. Chem. Phys. Discuss., 3, 551–596, 2003
www.atmos-chem-phys.org/acpd/3/551/

Atmospheric Chemistry and Physics Discussions

Atmospheric impact of the 1783–1784 Laki eruption: Part I Chemistry modelling

D. S. Stevenson[1], C. E. Johnson[2], E. J. Highwood[3], V. Gauci[4], W. J. Collins[2], and R. G. Derwent[2]

[1]Institute for Meteorology, University of Edinburgh, Edinburgh, UK
[2]Met Office, Bracknell, UK
[3]Department of Meteorology, University of Reading, UK
[4]Department of Earth Sciences, The Open University, UK

Received: 29 November 2002 – Accepted: 16 January 2003 – Published: 6 February 2003

Correspondence to: D. S. Stevenson (davids@met.ed.ac.uk)

Abstract

Results from the first chemistry-transport model study of the impact of the 1783–1784 Laki fissure eruption (Iceland: 64° N, 17° W) upon atmospheric composition are presented. The eruption released an estimated 122 Tg(SO_2) into the troposphere and lower stratosphere. The model has a high resolution tropopause region, and detailed sulphur chemistry. The simulated SO_2 plume spreads over much of the Northern Hemisphere, polewards of ~40° N. About 70% of the SO_2 gas is directly deposited to the surface before it can be oxidised to sulphuric acid aerosol. The main SO_2 oxidants, OH and H_2O_2, are depleted by up to 40% zonally, and the lifetime of SO_2 consequently increases. Zonally averaged tropospheric SO_2 concentrations over the first three months of the eruption exceed 20 ppbv, and sulphuric acid aerosol reaches ~2 ppbv. A total aerosol yield of 51–66 Tg(H_2SO_4) is produced. The mean aerosol lifetime is only 6–9 days, and the peak aerosol loading of the atmosphere is only ~7 Tg($H_2SO_4.2H_2O$). Due to the relatively short atmospheric residence times of both the SO_2 and sulphate, the aerosol loading approximately mirrors the temporal evolution of emissions associated with the eruption. The model produces a reasonable simulation of the acid deposition found in Greenland ice cores. These results appear to be relatively insensitive to the vertical profile of emissions assumed, although if more of the emissions reached higher levels (>12 km), this would give longer lifetimes and larger aerosol yields. This study suggests that most previous estimates of the global aerosol loading associated with Laki have been generally too large in magnitude, and too long-lived. Environmental effects following the Laki eruption may have been dominated by the widespread deposition of SO_2 gas rather than sulphuric acid aerosol.

1 Introduction

Large explosive volcanic eruptions of the past have significantly influenced Earth's climate (Robock, 2000). The crucial factor is not necessarily the magnitude of the erup-

tion, but is thought to be the quantity of sulphur dioxide (SO_2) injected into the stratosphere. Oxidation of the SO_2 generates sulphuric acid aerosol, which can persist for typically 1–2 years in the mid-stratosphere, and spread to cover much of the globe, as observed following the June 1991 Mt. Pinatubo eruption (Minnis et al., 1993). Stratospheric volcanic aerosol perturbs the planetary energy budget by reflecting sunlight, radiatively warming the aerosol layer, and cooling the underlying atmosphere, potentially affecting climate. Radiative perturbations can also generate significant dynamical feedbacks that may affect climate (Robock and Mao, 1992).

Eruptions that are mainly restricted to the troposphere are much less likely to alter climate, for two main reasons. Firstly, the SO_2 will not all be oxidised to aerosol, as gas deposition processes operate on similar timescales to oxidation. Secondly, the aerosol generated will be efficiently removed by deposition processes, and it will have a tropospheric lifetime of only days to weeks, compared with months to years in the stratosphere. However, if the volcanic SO_2 source is long-lived and sufficiently large, and if the emissions are efficiently oxidised to aerosol, then they also have the potential to significantly perturb the Earth's radiation budget and climate, in just the same way as present day anthropogenic SO_2 emissions (Penner et al., 2001).

In June 1783, a major Icelandic fissure eruption began, at a volcano that has subsequently become known as Laki. The eruption had several eyewitnesses, and was recorded in detail by Steingrímsson (1998). Thordarson and Self (2003) give a detailed description of the eruption. Over eight months, an estimated 15 km^3 of basaltic magma and 122 $Tg(SO_2)$ were emitted, with about 60% of this released during the first six weeks of the eruption (Thordarson et al., 1996). The eruption involved fire-fountaining of magma to an altitude up to 1.4 km, and this was topped by an ash cloud reaching to a maximum height of between 9 and 13 km, or around tropopause levels (~10 km over Iceland in summer). The eruption was one of the largest individual tropospheric pollution events of the last 250 years, and the quantity of SO_2 released was comparable to the total annual present-day anthropogenic input to the atmosphere: 142 Tg SO_2 in 1990 (Olivier et al., 1996). A dry fog was recorded over much of Europe during

the second half of the year (Stothers, 1996; Grattan and Pyatt, 1999), and similar phenomena were observed in Canada and China (Demaree et al., 1998), suggesting that a hemispheric-scale tropospheric sulphate aerosol cloud formed.

Ice-cores record large volcanic eruptions as acidic layers; the amount of acid deposited is used as a proxy for the aerosol loading caused by the eruption, and hence the likely climate impact (Robertson et al., 2001). Several studies of Greenland ice-cores have found evidence of the Laki eruption, in the form of an ash layer and a peak in sulphate (Clausen and Hammer, 1988; Fiacco et al., 1994; Zielinski, 1995; Clausen et al., 1997). Laj et al. (1990) found a depletion of hydrogen peroxide (H_2O_2) coincident with this sulphate peak. Fiacco et al. (1994) dated the ash layer from Laki as 1783, with the sulphate peak arriving a year later, indicating that the sulphate had remained airborne for about a year, implying a significant stratospheric aerosol layer formed. More recent Greenland ice-core studies (Clausen et al., 1997; Mosley-Thompson et al., 2002), however, place the sulphate peak in 1783, and indicate a much shorter lived, mainly tropospheric aerosol layer existed. The proximity of Greenland to Iceland raises the possibility that Icelandic eruptions may be more frequently recorded in the ice core record, and their magnitudes overestimated with respect to more distal eruptions (Zielinski, 1995). In particular, major Icelandic eruptions restricted to the troposphere may deposit large amounts of acid to Greenland, without necessarily generating a large-scale climate impact. Previous assessments of the aerosol generated by Laki (Thordarson et al., 1996; Stothers, 1996; Thordarson and Self, 2003) have assumed that all of the SO_2 released was converted to sulphuric acid aerosol. Thordarson et al. (1996) suggested that >75% of the emissions were injected at around tropopause levels, and that the aerosol generated remained aloft at these levels for over a year.

In this work, the impact on atmospheric composition resulting from the Laki eruption has been simulated for the first time using a global 3-D chemistry-transport model (CTM). The CTM simulates the formation, spread, and deposition of the aerosol, and the associated depletions of the oxidants (H_2O_2, OH, and O_3) that convert SO_2 to

sulphate. Other simulations of the model, for 1990 conditions and for pre-industrial conditions, provide baseline distributions of species to allow comparison of the model with recent observations and other models. Acid deposition to Greenland is simulated by the model, and is compared with ice-core records. The sulphate aerosol fields have been used in a complementary study (Highwood and Stevenson, 2003) to calculate radiative forcings and assess the climatic impact of the Laki eruption.

2 Chemistry-transport model

We used a new version of the UK Met Office 3-D Lagrangian CTM STOCHEM (Collins et al., 1997, 1999, 2000), developed at the University of Edinburgh (STOCHEM-Ed). The main improvements over previous versions are increased vertical resolution in both the driving general circulation model (GCM) and the CTM, particularly around the tropopause. STOCHEM-Ed is closely coupled to the Unified Model (UM) GCM (Johns et al., 1997), directly receiving meteorological fields every 3 h (Johnson et al., 2001). The UM was configured as an atmosphere-only GCM with a resolution of 3.75° longitude by 2.5° latitude, with 58 vertical levels between the surface and 0.1 hPa. Recent climatologies of sea-surface temperatures and stratospheric ozone were used.

Several aspects of STOCHEM have been compared with observations, including transport and mixing on short-timescales (Stevenson et al., 1998a) and long-timescales (Collins et al., 1998), and the magnitudes, distributions and seasonal variations of nitrogen oxides (NO_x), hydroxyl (OH) and peroxy (HO_2) radicals (Collins et al., 1999), carbon monoxide (CO) (Kanakidou et al., 1999a), ozone (O_3) (Kanakidou et al., 1999b), and aerosol species (Derwent et al., 2003). The model has also taken part in several intercomparisons regarding transport and chemistry (Olson et al., 1997; Isaksen et al., 1999; Rasch, 2000; Prather et al., 2001). In all these studies, STOCHEM typically performed well within the range of other current models.

2.1 Transport and mixing

STOCHEM-Ed uses a Lagrangian transport scheme, dividing the atmosphere into 50000 equal mass air parcels. These parcels are advected by winds from the GCM with a 4th order Runge-Kutta algorithm, using linear horizontal interpolation and cubic vertical interpolation, and adding a small random walk component to simulate diffusive mixing. The parcels maintain an approximately even global distribution with time. Convective mixing occurs between a fraction of the parcels beneath convective cloud tops, and inter-parcel mixing occurs between parcels occupying the same grid-box after each 1-h advection step. The grid used for mixing is 5° by 5°, with 22 vertical hybrid (η) levels (6 levels with $\Delta\eta$=0.1 between η=1.0 and η=0.4, 15 levels with $\Delta\eta$=0.025 between η=0.4 and η=0.025, and a top level between η=0.025 and η=0.0003). Hybrid co-ordinates are explained further in Collins et al. (1997), but can be considered as approximately equal to pressure divided by surface pressure. STOCHEM-Ed therefore has a vertical resolution of about 25 hPa around the tropopause. The same grid is used for data output, and 3-D emission fields, such as lightning NO_x and volcanic SO_2.

2.2 Chemical mechanism

Seventy chemical species are simulated, with a comprehensive description of tropospheric chemistry. Within each air parcel, these chemical species take part in 174 photochemical, gas-phase, and aqueous-phase chemical reactions, describing the chemistry of methane (CH_4), CO, NO_x, O_3, and 11 non-methane hydrocarbons (NMHC) (Collins et al., 1997, 1999). The scheme allows detailed calculation of diurnal and seasonal variations of oxidants, which are crucial to the sulphur chemistry.

The chemical mechanism also has a detailed description of several sulphur compounds, including dimethyl sulphide (DMS) oxidation (Jenkin et al., 1996) and aqueous-phase reactions. The main sulphur reactions and equilibria included are shown in Table 1. In the gas phase, reaction of SO_2 with OH is the main oxidation pathway. An important natural source of SO_2 and sulphuric acid aerosol (SA) is gas-phase oxida-

tion of DMS by OH in sunlight, and by the nitrate radical (NO_3) in darkness. Oceanic plankton are the main source of DMS, but there are also some emissions from soils.

Aqueous-phase oxidation of SO_2 is a major route for sulphate aerosol production (Langner and Rodhe, 1991). The model treats the aqueous-phase chemistry of several soluble species, including SO_2, ammonia (NH_3), nitric acid (HNO_3), H_2O_2 and O_3. In the presence of cloud water drops, gases are partitioned between gas and aqueous phases according to their Henry's Law coefficients. Compounds dissociate into their constituent ions in water. These two processes are rapid (Adams et al., 1999), and equilibrium is assumed. Reactions of HSO_3^- and SO_3^{2-} with H_2O_2 and O_3 to form sulphate (SO_4^{2-}) are significant SO_2 oxidation pathways. Any ammonium ions (NH_4^+) present combine with SO_4^{2-} ions to form ammonium sulphate aerosol ($(NH_4)_2SO_4$). The remaining sulphate ions form sulphuric acid aerosol. After each 5-min chemical timestep, aqueous and gas phase concentrations re-equilibrate.

One change to the chemistry in this model version is implementation of the conversion of dinitrogen pentoxide (N_2O_5) to nitrate aerosol (NAER) on sulphuric acid aerosol:

$$N_2O_5 \xrightarrow{SA} 2NAER \quad (1)$$

where the current model SA concentration field is used to calculate the rate constant ($k_1 = 5.0\times10^{-14}$[SA]), in a similar way to Dentener and Crutzen (1993). Previously, a fixed global rate constant was used for this reaction. Using the SA distribution to weight the reaction tends to reduce NO_x concentrations, particularly in polluted areas.

2.3 Emissions

Surface trace gas emissions are added to air parcels within the boundary layer above their sources. Gridded emission distributions with a horizontal resolution of $5^\circ \times 5^\circ$ are used. When several air parcels occupy the boundary layer for the grid square, emissions are divided equally between them. If no air parcels are present, emissions are stored until the next time-step, ensuring mass conservation.

Global annual emissions totals for various categories and gases are shown in Table 2. These values are for the 1990 scenario, but all the natural emissions (except volcanic SO_2 in the Laki scenarios) remain constant in all of the experiments. In the 1860 and Laki scenarios, anthropogenic emissions are set to zero, and biomass burning totals are reduced to 20% of their 1990 values (Stevenson et al., 1998b; Brasseur et al., 1998; Wang and Jacob, 1998; Mickley et al., 1999; Hauglustaine and Brasseur, 2001).

For the 1990 scenario, anthropogenic emissions distributions and totals from the EDGAR database (Olivier et al., 1996) are used. All anthropogenic categories except biomass burning are included, for NO_x, CO, CH_4, SO_2, NH_3, and NMHCs. We use the term anthropogenic for these lumped emissions that exclude biomass burning, although burning has both anthropogenic and natural components. The anthropogenic emissions have no seasonal variation.

For biomass burning, we use monthly varying magnitudes and distributions from Cooke and Wilson (1996), together with totals from IPCC OxComp (Prather et al., 2001). Emissions from vegetation (Guenther et al., 1995), soils (Yienger and Levy, 1995), wetlands, tundra (Matthews and Fung, 1987) and the oceans also vary monthly. Isoprene (C_5H_8) emissions from vegetation are linked to local solar zenith angle, as they are light and temperature sensitive. Four-dimensional (latitude-longitude-altitude-month) emissions of NO_x from lightning (Price and Rind, 1992) and aircraft (Isaksen et al., 1999) (for the 1990 case) are included.

Background volcanic SO_2 emissions total 8.8 $Tg(S)yr^{-1}$, based upon emissions for 1980 (Spiro et al., 1992). These data show peaks associated with the Mt. St. Helens eruption in 1980, and the continuous high SO_2 output from Mt. Etna on Sicily. Whilst volcanic emissions vary considerably in time and space (Andres and Kasgnoc, 1998), having spikes associated with eruptions, these emissions are thought to give a reasonable representation of the typical distributions and magnitudes of background volcanic emissions. The emissions are added to the model over the vertical range from the surface up to ~300 hPa, as most volcanic SO_2 is released during explosive eruptions

and from elevated sources, directly entering the free troposphere (Graf et al., 1997). The model's present-day sulphur cycle is analysed in more detail in Stevenson et al. (2003).

2.4 Dry and wet deposition

Within the boundary layer, dry deposition rates are calculated using species-dependent deposition velocities, the boundary layer height, and an effective vertical eddy diffusion coefficient derived from the surface stress, heat flux, and temperature. Deposition velocities vary between land, sea and ice, with values for SO_2 of 6, 8 and 0.5 mms^{-1} respectively, and values for sulphate (SA and $(NH_4)_2SO_4$) of 2, 1, and 0.05 mms^{-1}. Several other important species are dry deposited, including H_2O_2, O_3, NO_2 and NH_3.

Soluble species are subject to wet removal, through precipitation scavenging. This includes SO_2, sulphate, H_2O_2 and NH_3. Species-dependent scavenging rates are taken from Penner et al. (1994), and vary between dynamic and convective precipitation. Wash-out from dynamic precipitation only operates below ~400 hPa. Wet scavenging from convective clouds occurs when the precipitation rate exceeds 10^{-8} $kgm^{-2}s^{-1}$. The scavenging profile in convective clouds is constant below ~850 hPa, then decreases linearly to zero at the cloud top. Very little wet deposition occurs outside the tropics at altitudes above ~400 hPa.

2.5 Stratospheric ozone and stratosphere-troposphere exchange

Ozone is a gas crucial to tropospheric chemistry, and needs to be simulated realistically in order to accurately calculate other oxidants such as OH and H_2O_2. Several other studies with STOCHEM have focussed upon tropospheric O_3 (Collins et al., 1997, 2000; Stevenson et al., 1998b). The input of stratospheric O_3 is an important part of the tropospheric O_3 budget. Previous versions of STOCHEM only extended to ~100 hPa, and estimated the influx using vertical velocities and an O_3 climatology (Li and Shine, 1995) in the lower stratosphere. In this work, we impose this O_3 climatology

above the tropopause, and allow the advection scheme to transport O_3 downwards. To limit downwards mixing, no inter-air parcel mixing across the tropopause is allowed, so cross-tropopause transfer is achieved only through advection. Most current CTMs (Prather et al., 2001) parameterise or limit stratosphere-troposphere exchange (STE) to generate realistic influxes of O_3, because they lack tropopause resolution. However, because STOCHEM-Ed has a high resolution tropopause, we find that the source of stratospheric O_3 is realistic (~450 $Tg(O_3)\,yr^{-1}$) using the true advection. This suggests that STE in general should also be reasonable, and this will be important in realistically transporting volcanic emissions and their products in the tropopause region.

3 Experiments

Two years of meteorological data generated by the GCM were used to drive four repeat experiments with STOCHEM-Ed. These data did not vary between experiments, only the emissions changed. It should be noted that no attempt was made to simulate the meteorological conditions of 1783–1784. Synoptic daily weather maps of the 1780s over Europe have been constructed (Kington, 1978, 1988), and there is also evidence that a strong El Nino occurred during 1782–1783 (Ortlieb, 1993). Further simulations of the Laki eruption may benefit from the assimilation of this meteorological data, however this was not attempted here. Rather, we use the GCM to generate data representative of the 1990s. The results should not, therefore, be expected to simulate the observed day-by-day spread of the aerosol. However, they should indicate an approximate evolution of the aerosol cloud under a typical time-varying meteorology. Previous experiments using a different year's meteorology produced qualitatively similar results (Stevenson et al., 2001). Each integration started in September, and continued for 17 months. The first 4 months are considered as spin-up of STOCHEM-Ed, and are not used in the following analysis. The GCM is initialised from a dump for September 1996, and is already fully spun-up.

The four emission scenarios represented atmospheres of the present-day (1990),

the pre-industrial era (prior to c.1860), and two cases for the pre-industrial with the emissions from the Laki eruption superimposed. The two Laki simulations use the same magnitude and evolution of emissions, but apply different vertical profiles. In the first case (termed "Lo"), emissions are evenly distributed form the surface to ~300 hPa (~9 km). In the second ("Hi"), 25% of the SO_2 is emitted between the surface and ~700 hPa (~3 km), and 75% around tropopause levels (~300–175 hPa; ~9–13 km). The real vertical profile of emissions is unknown, but is probably more likely to resemble the "Hi" case, as most volcanic gases will be released during the most explosive phases of the eruption (which also reach the greatest altitudes), and are likely to be detrained from the top of the eruption cloud (Woods, 1993). A significant amount of SO_2 was also probably released close to the surface, directly from the fissures and lava flows. The split of 75%:25% was derived from preliminary modelling (S. Self, pers. comm., 2002), and is similar to the ratio of 80%:20% reported by Thordarson and Self (2003). The "Lo" case, with a higher proportion of gas released at lower levels, reflects the uncertainty in this split, the uncertainties in the actual heights of the eruption clouds, and the possibility that some of the gas could be detrained before reaching the cloud top. As such, the "Lo" case probably represents the lowest reasonable range of altitudes for the SO_2 emission.

For the Laki simulations, we added an extra source of SO_2 to the grid over Iceland, using the emissions estimated by Thordarson et al. (1996), which total 61 Tg(S). Thordarson et al. (1996) described the evolution of the eruption, and estimated the associated SO_2 emissions using the "petrologic method". This technique takes advantage of the fact that glass inclusions, trapped within phenocrysts in the lava, represent samples of undegassed magma. By analysing the sulphur content of these inclusions, together with the sulphur content of degassed lava, the quantity of sulphur released per unit volume of magma erupted was deduced. This method is generally accepted to give a minimum for the gas released upon eruption (Wallace, 2001). Using historical data from observations, the variation of the eruption rate with time was also estimated. These two quantities yield the time evolution of the sulphur emissions. We used

monthly mean emissions in the simulation, and added them between 1 June and 31 January, rather than the actual dates of the eruption (8 June 1783 to 7 February 1784). Thordarson et al. (1996) estimated that 60% of the SO_2 was released in the first 1.5 months, a further 30% over the next 3.5 months, and the remaining 10% during the final 3 months. These figures translate to 0.80 Tg(S)day^{-1} in June, 0.49 Tg(S)day^{-1} in July, 0.35 Tg(S)day^{-1} between August and October, and 0.14 Tg(S)day^{-1} from November to the end of January. The eruption was quite strongly episodic, featuring 10 episodes, each 0.5 to 3 days long, over the first 5 months, with inter-episode repose periods of 3 to 30 days (Thordarson and Self, 2003). Most of the gas was likely to have been released during the most explosive phases of the eruption, so using monthly mean emissions is an approximation. However, the lifetimes of SO_2 and SO_4 are probably sufficiently long that this wouldn't have a significant impact on the monthly to seasonal mean results analysed here.

4 Results and discussion

4.1 Sulphur dioxide and oxidants

Figure 1 shows zonal June–July–August (JJA) mean SO_2 for 1990, 1860, and the two Laki experiments. Table 3 shows annual mean and JJA global budgets for SO_2 and sulphate for the three experiments, showing the figures for Laki relative to 1860. For the 1990 scenario, annual SO_2 emissions total 81.3 Tg(S), from anthropogenic, volcanic, and biomass burning sources. A further 11.7 Tg(S)yr^{-1} comes from the oxidation of DMS, yielding a total annual SO_2 source of 93 Tg(S). The 1860 scenario has the same volcanic source, 20% of the biomass burning source, and no anthropogenic source. The 1860 DMS source remains the same, but slightly more SO_2 is generated from it, due to small changes in the DMS oxidation chemistry. The Laki scenarios are the same as the 1860 scenario, with the addition of 61.3 Tg(S) over Iceland for the 8 months June to January.

In the 1990 scenario, 41% of the SO_2 is deposited to the surface, predominantly by dry deposition. The remaining SO_2 is converted to sulphate aerosol, partly by gas-phase OH oxidation (6%), but mainly by aqueous-phase oxidation, through the reactions involving H_2O_2 (34%) and O_3 (18%). The total SO_2 atmospheric burden is 0.29 Tg(S), and dividing this by the total loss rate gives a global annual mean lifetime (τ_{SO_2}) of 1.1 days. Several recent model studies of the present-day tropospheric sulphur cycle are reviewed by Koch et al. (1999), and have burdens in the range 0.20–0.61 Tg(S) and lifetimes of 0.6–2.6 days. Results from STOCHEM-Ed are towards the lower end of these ranges. Figure 2a shows the zonal JJA mean τ_{SO_2} for 1990, calculated from the zonal mean SO_2 distribution (Fig. 1a) and the zonal mean total loss rate for SO_2, from both oxidation and deposition. Lifetimes range from 0.2 days in the marine boundary layer of the Southern oceans to over 50 days in the polar upper troposphere (UT). One reason for the increase in lifetime with altitude is the general decrease in abundance of clouds with altitude in the free troposphere, limiting the aqueous oxidation pathway. In the tropics, τ_{SO_2} is under 2 days almost throughout the troposphere. At Icelandic latitudes, τ_{SO_2} lengthens from about 0.5 days at the surface to over 10 days in the UT. The short lifetime of SO_2 leads to steep gradients in concentration around the source regions and low concentrations at sites remote from these emissions (Fig. 1a).

In the 1860 scenario, where much of the SO_2 originates from volcanoes and is released at higher altitudes, a smaller fraction (19%) is deposited. Compared to 1990, a slightly larger fraction goes through the H_2O_2 oxidation route rather than the O_3 reaction. Both O_3 and H_2O_2 were lower in pre-industrial times, but whilst H_2O_2 increases since 1860 have been centred on the tropics, O_3 increases have been mainly in the Northern Hemisphere (NH), co-located with the rising industrial SO_2 emissions. This explains the greater importance of the O_3 oxidation path in the 1990 simulation. The 1860 SO_2 burden is 33% of the 1990 value, and its global annual mean lifetime is 1.6 days (44% longer than in 1990). Figure 2b reveals a slightly shorter SO_2 lifetime near the surface in 1860 compared to 1990, but a longer lifetime in the free troposphere. The longer globally averaged lifetime reflects both the higher mean altitude of emis-

sions, and the lower levels of the main oxidants at these levels. Figure 1b shows the SO_2 distribution for JJA 1860. When compared with Fig. 1a, many similar features can be seen, particularly in the tropics and the SH. These are due to the common natural emissions' sources in these two scenarios. The peak values in the pre-industrial NH are mainly due to volcanic emissions from Italy, N. America, Iceland and E. Asia.

Figures 1c–d show JJA SO_2 distributions for the two Laki cases. This shows that Laki enhanced summer SO_2 zonally by over 20 ppbv, with concentrations over 100 times higher than peak values in 1860. Large increases in SO_2 are seen polewards of ~30° N. In the Laki Lo case, the SO_2 pertubation is limited to the troposphere, but in the Laki Hi case, some of the high level emissions are transported equatorwards in the lower stratosphere (LS). Longer SO_2 lifetimes at altitude generate higher SO_2 concentrations, particularly polewards of 60° N. Lower tropospheric concentrations are similar in both cases.

By looking at the difference in the budgets between the Laki and 1860 scenarios, we can see the simulated fate of the SO_2 emitted by Laki. Most (64–72%) of the emitted SO_2 is deposited to the surface, roughly equally divided between wet and dry deposition. The remaining SO_2 is converted to aerosol, with about half being oxidised in the gas-phase, the rest mainly through the H_2O_2 reaction. This is in contrast to the 1860 atmosphere, where aqueous-phase oxidation dominates over deposition and gas-phase oxidation. Comparing the Laki and 1860 scenarios for JJA, oxidation in the gas-phase increases by a factor of 13–14, but in the aqueous-phase only increases by a factor of 2.3–2.7. The high levels of SO_2 causes depletion of its oxidants (Fig. 3). H_2O_2 is most strongly affected, and aqueous-phase oxidation approaches saturation more rapidly than gas-phase oxidation. The largest depletions in H_2O_2, of over 30% in the zonal JJA field, occur in the cloudy storm-track regions (50–65° N). OH depletion reaches 18%, and is co-located with the regions of SO_2 increase (Fig. 1). Over the relatively cloud-free Arctic, H_2O_2 shows small increases, due to a chemical feedback associated with the OH depletion. Tropospheric ozone is also slightly reduced (typically by 1–2%), but this is mainly related to lowering of NO_x associated with the elevated aerosol con-

centrations (Eq. 1), rather than chemical reaction with dissolved SO_2. These oxidant depletions cause increases in τ_{SO_2} (Fig. 2c–d). The lifetime of the Laki SO_2 is 9–16 days, over 5 times the background 1860 value (Table 3). These increases are partly due to the fact that the Laki emissions are in a region of the atmosphere where τ_{SO_2} is greater than the global mean value, and partly because oxidants are depleted by the massive SO_2 injection.

The average lifetime of the Laki SO_2 appears to be surprisingly short, given the SO_2 distributions (Fig. 1) and the zonal mean lifetime (Fig. 2). However, the relatively short lifetime towards the surface tends to dominate the calculation, and limits the concentration increases seen here. In addition, transport from the UT and LS can move SO_2 into regions where lifetimes are shorter.

4.2 Sulphate

Sulphate is the product of SO_2 oxidation; there is also an insignificant pathway direct from DMS (Table 1). Sulphate is partitioned into two species in the model: ammonium sulphate and sulphuric acid. In the 1990 scenario, the relatively high anthropogenic emissions of NH_3 mean that over half the sulphate burden exists as ammonium sulphate. In the 1860 scenario, NH_3 emissions were lower, and only about a third of the sulphate was ammonium sulphate. The extra sulphate formed following the Laki eruption is almost exclusively sulphuric acid aerosol, as there are very few free ammonium ions. Sulphate distributions (Fig. 4) are smoother and more widespread than their precursor, reflecting the longer sulphate lifetime. Laki sulphate levels reach 1–2 ppbv over much of the summer troposphere polewards of ~50° N, compared to 1990 levels of 300–500 pptv in NH mid-latitudes.

The only sinks for sulphate are deposition, and wet deposition dominates over dry. Dry deposition only operates in the boundary layer, but wet scavenging occurs throughout and beneath precipitating clouds. The local sulphate lifetime (τ_{SO_4}) is therefore determined by purely physical processes, and is invariant between all four scenarios (Fig. 5). In the UT outside the tropics there are less clouds, and the effective lifetime

in these regions is controlled by the timescale of transport into regions where sinks do operate. Global mean τ_{SO_4} do vary between scenarios, as they also reflect the sulphate distribution. The 1990 scenario has a global annual mean τ_{SO_4} of 5.4 days, and a burden of 0.81 Tg(S). Like SO_2, these values fall within the ranges found in previous modelling studies: τ_{SO_4}: 3.9–5.7 days; sulphate burden: 0.53–0.96 Tg(S) (Koch et al., 1999). Mean sulphate lifetimes for the Laki cases are up to 9.1 days, as a significant fraction of the sulphate is in the UT/LS where the local lifetime is relatively long.

4.3 Comparison of the 1990 scenario with observations

Figure 6 shows monthly mean modelled SO_2 and sulphate from the 1990 experiment, and observed values from three European stations: Spitzbergen in the Arctic; Tange in central Europe; and Roquetas in SW Europe (Hjellbrekke et al., 1996). The figure shows model results for 17 months (the full run length, excluding the first 4 months spin-up), with 12 months of observations. Differences in the intitial and final 5 months indicate interannual variability arising from the meteorology, which is quite large for these relatively short-lived species. At all three sites, the magnitudes and seasonal cycle of sulphate and SO_2 are reasonably reproduced, although SO_2 is slightly less well modelled. Over central Europe, SO_2 is over-estimated by the model, typically by a factor of over two. At Spitzbergen and Roquetas, the SO_2 cycle is modelled better, but there are significant differences in several months. These problems are probably related to the resolution of the model, and in particular the coarse (5° × 5°) emissions grid over Europe. In addition, the use of meteorological data from a climate model, rather than analysed data, will mean that cloud and precipitation distributions, winds and boundary layer heights may not be representative of the conditions prevailing when observations were taken. These factors, combined with the short lifetime of SO_2, make it a particularly difficult gas to compare with measurements. Despite these problems with SO_2, which are typical of models (Restad et al., 1998; Koch et al., 1999), the reasonable agreement with sulphate is encouraging, and gives us confidence in the results. A more detailed validation of sulphur species in the model is presented by

Derwent et al. (2003).

Also plotted on Fig. 6 are the modelled results from the background pre-industrial run, and the two Laki scenarios, with the results scaled to fit on the plots. These show the major influence of the eruption on European air quality during the summer of 1783, and the likely impact of a similar eruption today.

4.4 Temporal evolution of the Laki impact

Given the relatively short lifetimes of both SO_2 and sulphate in the troposphere, the temporal evolution of the Laki eruption impact is mainly controlled by the variation with time of the emissions. Figure 7 shows the evolution of the zonal mean sulphate from Laki in the model, for the surface, UT, and LS. The impact of the eruption is essentially restricted to the NH, with only a small amount of transport into the SH in the LS. Sulphate peaks in the second month of the eruption (July). In the lower troposphere, as soon as the emissions shut off in February, the anomaly ceases. This is also mainly true of the UT/LS, although the longer sulphate lifetime in this region allows a minor perturbation to persist for a few months.

4.5 Sulphur deposition

Annual total sulphur deposition fields for the four cases are shown in Fig. 8. Total sulphur deposition is the sum of wet and dry deposition of SO_2, H_2SO_4 and $(NH_4)_2SO_4$. Annual totals for each process are given in Table 3. Much of the sulphur is dry deposited as SO_2 gas; wet deposition of SO_2 is unlikely to be distingushable from wet deposition of H_2SO_4 aerosol. Present-day deposition peaks over the three industrial centres, but is many times higher than pre-industrial levels over much of the NH. Much of the Laki sulphur was deposited over Iceland, but large amounts also reached northern Europe and Asia. Acid deposition from sulphur and other volcanic volatiles, including HF and HCl, is thought to have been responsible for the crop damage and livestock deaths in Iceland and the famine that followed the eruption. Away from regions of signif-

icant rainfall, environmental effects from sulphur deposition following the eruption may have been dominated by the widespread deposition of SO_2 gas rather than sulphuric acid aerosol.

Figure 9 shows modelled monthly total sulphur and H_2SO_4 deposition fluxes to a grid-square in central Greenland for the two Laki cases. Sulphur deposition increases by ~2 orders of magnitude above background levels at the start of the eruption, but rapidly declines to normal levels once the eruption ends. Peak modelled fluxes reach ~200 $mg(S)m^{-2}month^{-1}$. The majority (~85%) of the sulphur is deposited as SO_2 rather than H_2SO_4. Modelled sulphur deposition to Greenland over the year following the eruption totals 360–500 $mg(S)m^{-2}$, compared to background levels of ~8.6 $mg(S)m^{-2}$ in 1860 and roughly double that value in 1990. There is no indication in either simulation of a peak in the following spring, as suggested by one ice core study (Fiacco et al., 1994). Instead, these model results support later ice-core studies (Mosley-Thompson et al., 2002) that indicate a sulphate peak in 1783, coincident with the eruption.

Table 4 shows measured H_2SO_4 accumulations in several Greenland ice cores (Clausen and Hammer, 1988; Zielinski, 1995; Clausen et al., 1997; Mosley-Thompson et al., 2002), compared to our model results. Modelled background values, and the total H_2SO_4 deposition associated with the eruption, are both in reasonable agreement with measurements. This suggests that the deposited SO_2 was not oxidised to SO_4^{2-} after deposition; possibly it was re-emitted, or preserved as SO_2 and just not measured by any of the techniques applied in the ice-core analyses. Any re-emission of SO_2 from snow would further enhance SO_2 concentrations in the lower troposphere.

4.6 Total aerosol yield and peak atmospheric loading

The modelled global atmospheric burden of H_2SO_4 rises from background levels of ~0.5 Tg to ~5 Tg in July, followed by an approximately exponential decay back to normal values over the next 12 months (Fig. 10). In the Laki Hi case, the decay is slower, and slightly elevated levels of ~0.8 Tg still exist after a year. The total atmospheric

aerosol mass is likely to be 37% higher than these values, as H_2SO_4 typically exists as $H_2SO_4.2H_2O$. This indicates a peak global aerosol loading of ~7 Tg, similar to the estimate of Stothers (1996).

Table 5 compares our model results with previous estimates of the total aerosol yield from Laki, either derived from Greenland ice core deposits (Clausen and Hammer, 1988; Zielinski, 1995; Clausen et al., 1997), or from observed optical depths (Stothers, 1996), or inferred from emissions (Thordarson et al., 1996; Thordarson and Self, 2003). The largest estimate is from Clausen and Hammer (1988) who used ice core measurements together with measured deposition of nuclear bomb products from a high Northern latitude test of known magnitude, to infer an atmospheric aerosol loading for Laki of 280 Tg(H_2SO_4).

Our work indicates total aerosol production from Laki of 51–66 Tg(H_2SO_4). Due to the relatively short atmospheric lifetime of the aerosol, its peak burden is only ~5 Tg(H_2SO_4) (Fig. 10), as discussed above. The Clausen and Hammer (1988) overestimate occurs mainly because Laki was much closer to Greenland than the nuclear test, and added material to the atmosphere at lower altitudes.

4.7 Missing feedbacks and other uncertainties

The model results presented here represent a new approach compared with previous assessments of the atmospheric impact from the Laki eruption. However, there remain large uncertainties in the results. Several potentially important couplings have not been included in the simulations described here. The modelled aerosol does not influence the model photolysis rates, which are important in determining oxidant concentrations (Tie et al., 2001). There is also no dynamical feedback of the aerosol on the model's meteorology, either through the radiation code or through the cloud scheme. However, the climatic impact of the aerosol is examined using a decoupled methodology in the second part of this work (Highwood and Stevenson, 2003). Possibly the largest uncertainty associated with the Laki eruption is the height profile of the SO_2 emissions. We have used two different profiles in an attempt to span a wide range of possibil-

ities. Nevertheless, the SO_2 could have been predominantly emitted at either lower or higher altitudes than used here. Higher level emissions may have been oxidised more efficiently and remained airborne for a longer period than calculated here. For lower altitude emissions the reverse would be true. The estimated emissions only represent a minimum total magnitude. On the other hand, no attempt has been made to model chemistry in the volcanic plume, and there may have been significant removal of sulphur from the system, for example by uptake on ash particles. The broadly similar conclusions reached for both the Laki Lo and Laki Hi scenarios suggests that the vertical profile may not be a crucial factor. The episodicity of the eruption has also been neglected, and this may modulate the results somewhat. However, the similar timescales of the episodes (days to weeks) and the chemical lifetimes of SO_2 and SO_4 suggest that this will not significantly alter the results, particularly when averaged over monthly, seasonal or annual periods.

Another possible impact on atmospheric composition that we have neglected involves the effect of sulphur deposition from Laki upon the global source of methane, which may have been significantly reduced. Recent findings show that levels of sulphur deposition comparable to those reported here can significantly reduce CH_4 emissions from natural freshwater wetlands and tundra (Gauci et al., 2002). An increase in the sulphate supply to these areas is thought to stimulate microbial competition in anaerobic soils by enabling sulphate-reducing bacteria to out-compete methane-producing micro-organisms for available substrates (Lovely and Klug, 1983). Wetlands and tundra formed the major pre-industrial CH_4 sources, with the highest concentration located in mid to high northern latitudes (Matthews and Fung, 1987). It is likely that many of these CH_4 sources, and in particular those in Scandinavia and Siberia, will have been sufficiently impacted by the sulphur deposited from Laki for atmospheric CH_4 levels to have been reduced. These effects may have continued well beyond the period of the eruption, possibly for several years. Perturbations to atmospheric CH_4 are known to decay with decadal timescales (Prather, 1994; Derwent et al, 2001), so this process could introduce a relatively long-lived climate impact. Further investigation of these

mechanisms and uncertainties is beyond the scope of this paper and requires further research.

4.8 Implications for similar eruptions

Eruptions similar to Laki have a return period of a few hundred years, for example the Eldgjá eruption from Iceland in the tenth century (Stothers, 1998). A similar eruption today would add to anthropogenic pollution, and could pose major air quality problems in terms of SO_2 and particle concentrations (Fig. 6). It may also provide an opportunity to observe the troposphere under a very high aerosol load, possibly revealing details about the direct and indirect affects of aerosols, an area of high uncertainty in models of future climate change (Penner et al., 2001).

These results also have implications for the similar, but much larger, flood basalt eruptions of the geological past, e.g. the Roza eruption (Thordarson and Self, 1996). Previous studies of these have generally assumed that all of the SO_2 released went on to form aerosol, and hence affect climate. At much larger SO_2 loadings than Laki, oxidant depletion in the troposphere is likely to be even more intense (although this may depend on the latitude and season of the eruption), and an even higher proportion of the SO_2 will be deposited rather than form aerosol. The environmental effects of widespread SO_2 deposition (Grattan, 1998) may outweigh climate perturbations, and may also affect temperature proxies such as tree-rings (Pearson et al., 2002). Volcanic aerosols formed in the troposphere or LS should not be assumed to have atmospheric residence times similar to the 1991 Mt. Pinatubo aerosol (1–2 years), which was injected to heights of 20–25 km. A recent study by Blake (2003) suggests that historical explosive eruptions only generated a significant climate impact if they injected material to altitudes of 1.5 times the local tropopause height. At these altitudes, the aerosol will have a residence time similar to the Mt. Pinatubo aerosol, but at lower heights, aerosol will be removed more rapidly.

This modelling study has some deficiencies in its treatment of the LS (e.g. lack of complete stratospheric chemistry), however it suggests that we should exercise caution

when considering the climate effects of eruptions that only reach the LS, as aerosol residence times in this region may not be sufficiently long to significantly perturb climate. On the other hand, if the eruption is long enough in duration, then sustained SO_2 emissions may generate tropospheric aerosol with potential to affect climate, in just the same way as present-day anthropogenic SO_2 emissions.

5 Conclusions

Simulations of the global tropospheric sulphur cycle with a 3-D chemistry-transport model have been performed for 1990, 1860, and during the 1783–1784 Laki eruption. Sulphate and SO_2 budgets and concentrations from the present-day case compare well with observations and other state-of-the-art models. The model allows the fate of the SO_2 emitted by Laki to be analysed in detail. Peak zonal mean concentrations during the summer of 1783 are ~20 ppbv SO_2 and ~2 ppbv SO_4^{2-}. About 70% of the volcanic SO_2 is deposited before it has the chance to form aerosol. The remaining SO_2 is oxidised by OH in the gas-phase and mainly by H_2O_2 in the aqueous-phase, causing a significant depletion in both of these oxidants. This oxidant depletion significantly increases the local lifetime of SO_2, and the mean lifetime of Laki SO_2 is 9–16 days. The model generates a total of 51–66 Tg(H_2SO_4) from the eruption, with a mean lifetime of 6–9 days. The peak total aerosol loading of the atmosphere is ~7 Tg($H_2SO_4.2H_2O$), generally much lower than previous estimates. In the lower stratosphere, aerosol has a longer lifetime, but most of the aerosol generated has been removed by the end of the eruption. Simulated deposition of H_2SO_4 to central Greenland is in reasonable agreement with measurements, and approximately coincides with the eruption. These results have implications for large-scale volcanic eruptions that add large quantities of SO_2 to the troposphere and lower stratosphere. Some previous studies have wrongly assumed that most of this SO_2 will form aerosol with relatively long atmospheric residence times. This study suggests that much of the SO_2 will be deposited before oxidation, and that aerosol residence times will be of the order of weeks, rather than the

commonly assumed 1–2 years, which is more appropriate for large explosive eruptions that add material to the mid-stratosphere.

Acknowledgements. We would like to thank T. Crowley and E. Mosley-Thompson for providing advice and ice core data. DSS was funded by a NERC UGAMP fellowship and a NERC/Environment Agency advanced fellowship (P4-F02). EJH was partly funded by a NERC fellowship. CEJ, WJC and RGD thank DETR for support through contracts EPG 1/3/164 and PECD 7/12/37.

References

Adams, P. J., Seinfeld, J. H., and Koch, D. M.: Global concentrations of tropospheric sulphate, nitrate, and ammonium aerosol simulated in a general circulation model, J. Geophys. Res., 104, 13791–13823, 1999. 557

Andres, R. J. and Kasgnoc, A. D.: A time-averaged inventory of subaerial volcanic sulfur emissions, J. Geophys. Res., 103, 25251–25261, 1998. 558

Blake, S.: Correlations between eruption magnitude, SO_2 yield, and surface cooling, in: Volcanic degassing: Experiments, Models, Observations and Impacts, eds. Oppenhiemer, C., Pyle, D., and Barclay, J., Geol. Soc. Spec. Pub., in press, 2003. 571

Brasseur, G. P., Kiehl, J. t., Müller, J. F., Schneider, T., Granier, C., Tie, X. X., and Hauglustaine, D.: Past and future changes in global tropospheric ozone: Impact on radiative forcing, Geophys. Res. Lett., 25, 3807–3810, 1998. 558

Clausen, H. B. and Hammer, C. U.: The Laki and Tambora eruptions as revealed in Greenland ice cores from 11 locations, Annals of Glaciology, 10, 16–22, 1988. 554, 568, 569, 585, 586

Clausen, H. B., Hammer, C. U., Hvidberg, C. S., Dahl-Jensen, D., Steffensen, J. P., Kipfstuhl, J., and Legrand, M.: A comparison of the volcanic records over the past 4000 years from the Greeland Ice Core Project and Dye 3 Greenland ice cores, J. Geophys. Res., 102, 26707–26723, 1997. 554, 568, 569, 585, 586

Collins, W. J., Stevenson, D. S., Johnson, C. E., and Derwent, R. G.: Tropospheric ozone in a global-scale 3-D Lagrangian model and its response to NO_x emission controls, J. Atmos. Chem., 26, 223–274, 1997. 555, 556, 559

Collins, W. J., Stevenson, D. S., Johnson, C. E., and Derwent, R. G.: A simulation of long-range

transport of CFCs in the troposphere using a 3-D Global Lagrangian model with 6-hourly meteorological fields, Air Pollution Modeling and Its Application XII, 227–235, 1998. 555

Collins, W. J., Stevenson, D. S., Johnson, C. E., and Derwent, R. G.: Role of convection in determining the budget of odd hydrogen in the upper troposphere, J. Geophys. Res., 104, 26927–26941, 1999. 555, 556

Collins, W. J., Derwent, R. G., Johnson, C. E., and Stevenson, D. S.: The impact of human activities upon the photochemical production and destruction of tropospheric ozone, Q. J. R. Meteorol. Soc., 126, 1925–1952, 2000. 555, 559

Cooke W. F. and Wilson, J. J. N.: A global black carbon aerosol model, J. Geophys. Res., 101, 19395–19409, 1996. 558

Demaree, G. R., Ogilvie, A. E. J., and Zhang, D.: Further documentary evidence of northern hemispheric coverage of the great dry fog of 1783, Climatic Change, 39, 727–730, 1998. 554

Dentener, F. J. and Crutzen, P. J.: Reaction of N_2O_5 on tropospheric aerosols: Impact on the global distribution of NO_x, O_3 and OH, J. Geophys. Res., 98, 7149–7163, 1993. 557

Derwent, R. G., Collins, W. J., Johnson, C. E., and Stevenson, D. S.: Transient behaviour of tropospheric ozone precursors in a global 3-D CTM and their indirect greenhouse effects, Climatic Change, 49, 463–487, 2001. 570

Derwent, R. G., Collins, W. J., Jenkin, M. E., Johnson, C. E., and Stevenson, D. S.: The global distribution of secondary particulate matter in a 3-D Lagrangian chemistry transport model, J. Atmos. Chem., in press 2003. 555, 567

Fiacco, R. J., Thordarson, T., Germani, M. S., et al.: Atmospheric aerosol loading and transport due to the 1783–1784 Laki eruption in Iceland, interpreted from ash particles and acidity in the GISP2 ice core, Quaternary Research, 42, 231–240, 1994. 554, 568

Gauci, V., Dise, N. B., and Fowler, D.: Controls on suppression of methane flux from a peat bog subjected to simulated acid rain sulfate deposition, Glob. Biogeochem. Cycles, 16, 1, 10.1029/2000GB001370, 2002. 570

Graf, H.-F., Feichter, J., and Langmann, B.: Volcanic sulfur emission: Estimates of source strength and its contribution to the global sulfate distribution, J. Geophys. Res., 102, 10727–10738, 1997. 559

Grattan, J. P.: The distal impact of volcanic gases and aerosols in Europe: a review of the 1783 Laki fissure eruption and environmental vulnerability in the late 20th century, Geological Society Special Publication, 15, 9, 7–53, 1998. 571

Grattan, J. P. and Pyatt, F. B.: Volcanic eruption dry fogs and the European palaeoenvironmental record: localised phenomena or hemispheric impacts? Global and Planetary Change, 21, 173–179, 1999. 554

Guenther, A., Hewitt, C., Erickson, D., et al.: A global model of natural volatile organic compound emissions, J. Geophys. Res., 100, 8873–8892, 1995. 558

558

Hauglustaine, D. A. and Brasseur, G. P.: Evolution of tropospheric ozone under anthropogenic acitvities and associated radiative forcing of climate, J. Geophys. Res., 106, 32337–32360, 2001.

Highwood, E. J. and Stevenson, D. S.: Atmospheric impact of the 1783–1784 Laki eruption: Part 2 Climatic effect of sulphate aerosol, Atm. Chem. Phys. Disc., submitted, 2003. 555, 569

Hjellbrekke, A.-G., Schaug, J., and Skjelmoen, J. E.: EMEP Data Report 1994, Part 1: Annual summaries, EMEP/CCC Report 4/96, Norwegian Institute for Air Research, Kjeller, Norway, 1996. 566, 592

Isaksen, I., Jackman, C., Baughcum, S., et al.: Modeling the chemical composition of the future atmosphere, in: Aviation and the Global Atmosphere, Penner, J. E. et al. (eds.), Cambridge University Press, Cambridge, UK and New York, NY, USA, 373, 1999. 555, 558

Jenkin, M. E., Clement, C. F., and Ford, I. J.: Gas-to-particle conversion pathways, AEA Technology Report, AEA/RAMP/20010010/001/Issue 1, Culham Laboratory, Oxfordshire, UK, 1996. 556

Johns, T. C., Carnell, R. E., Crossley, J. F., et al.: The Second Hadley Centre Coupled Ocean-Atmosphere GCM: Model Description, Spinup and Validation, Clim. Dyn., 13, 103–134, 1997. 555

Johnson, C. E., Stevenson, D. S., Collins, W. J., and Derwent, R. G.: Role of climate feedback on methane and ozone studied with a coupled Ocean-Atmosphere-Chemistry model, Geophys. Res. Lett., 28, 1723–1726, 2001. 555

Kanakidou, M., Dentener, F. J., Brasseur, G. P., et al.: 3-D global simulations of tropospheric CO distributions – Results of the GIM/IGAC intercomparison 1997 exercise, Chemosphere: Global Change Science, 1, 263–282, 1999a. 555

Kanakidou, M., Dentener, F. J., Brasseur, G. P., et al.: 3-D global simulations of tropospheric chemistry with focus on ozone distributions, Eur. Comm. Rep., EUR18842, 1999b. 555

Kington, J. A.: Historical daily synoptic weather maps from the 1780s, J. Meteorol., 3, 65–70,

1978. 560

Kington, J. A.: The weather of the 1780s over Europe, Cambridge University Press, Cambridge, England, 164, 1988. 560

Koch, D. M., Jacob, D., Tegen, I., Rind, D., and Chin, M.: Tropospheric sulfur simulation and sulfate direct radiative forcing in the Goddard Institute for Space Studies general circulation model, J. Geophys. Res., 104, 23799–23822, 1999. 563, 566

554

Laj, P., Drummey, S. M., Spencer, M. J., et al.: Depletion of H_2O_2 in a Greenland ice core: implications for oxidation of volcanic SO_2, Nature, 346, 45–48, 1990.

Langner, J. and Rodhe, H.: A global three-dimensional model of the tropospheric sulphur cycle, J. Atmos. Chem., , 13, 225–263, 1991. 557

Li, D. and Shine, K. P.: A 4-D ozone climatology for UGAMP models, UGAMP internal report No. 35, 19, Dept. Meteorology, Univ. Reading, UK, 1995. 559

Lovely, D. R. and Klug, M. A.: Sulfate reducers can outcompete methanogens at freshwater sulfate concentrations, Appl. Environ. Microbiol., 45, 1, 187–192, 1983. 570

Matthews, E. and Fung, I.: CH_4 emissions from natural wetlands: Global distribution, area and environmental characteristics of sources, Glob. Biogeochem. Cycles, 1, 1, 61–86, 1987. 558, 570

Mickley, L. J., Murti, P. P., Jacob, D. J., Logan, J. A., Koch, D. M., and Rind, D.: Radiative forcing from tropospheric ozone calculated with a unified chemistry-climate model, J. Geophys. Res., 104, 30153–30172, 1999. 558

Minnis, P., Harrison, E. F., Stowe, L. L., et al.: Radiative climate forcing by the Mount Pinatubo eruption, Science, 259, 1411–1415, 1993. 553

Mosley-Thompson, E., Mashiotta, T. A., and Thompson, L. G.: Ice core records of late Holocene volcanism: Contributions from the Greenland PARCA cores, Volcanism and the Earth's Atmosphere, AGU Chapman Conference proceedings, 2002. 554, 568, 585

Olivier, J. G. J., Bouwman, A. F., van der Maas, C. W. M., et al.: Description of EDGAR Version 2.0, RIVM report No. 771060 002, RIVM, Bilthoven, 1996. 553, 558

Olson, J., Prather, M., Berntsen, T., et al.: Results from the Intergovernmental Panel on Climatic Change photochemical model intercomparison (PHOTOCOMP), J. Geophys. Res., 102, 5979–5991, 1997. 555

Ortlieb, L. and Machare, J.: Former El Nino events – records from Western South America Global Planetary Change, 7, 1–3, 181–202, 1993. 560

Pearson, C., Manning, S., Coleman, M., and Jarvis, K.: Volcanic eruptions, tree rings and multielemental chemistry: In search of an absolute date for volcanic eruptions of the prehistoric, Volcanism and the Earth's Atmosphere, AGU Chapman Conference proceedings, 2002. 571

Penner, J. E., Atherton, C. S., Dignon, J., Ghan, S. J., Walton, J. J., and Hameed, S.: Global emissions and models of photochemically active compounds, in Global Atmospheric Biospheric Chemistry, edited by R. G. Prinn, 223–247, Plenum, New York, 1994. 559

Penner, J. E., Andreae, M., Annegarn, H., et al.: Aerosols, their direct and indirect effects, In: Climate Change 2001: The Scientific Basis. Contribution of Working Group I to the Third Assessment Report of the Intergovernmental Panel on Climate Change, Houghton, J. T. et al. (eds.), Cambridge University Press, Cambridge, UK and New York, NY, USA, 881, 2001. 553, 571

Prather. M. J.: Lifetimes and eigenstates in atmospheric chemistry, Geophys. Res. Lett., 21, 801–804, 1994. 570

Prather, M. J., Ehhalt, D., Dentener, F., et al.: Atmospheric chemistry of greenhouse gases, In: Climate Change 2001: The Scientific Basis. Contribution of Working Group I to the Third Assessment Report of the Intergovernmental Panel on Climate Change [Houghton, J. T. et al. (eds.), Cambridge University Press, Cambridge, UK and New York, NY, USA, 881, 2001. 555, 558, 560

Price, C. and Rind, D.: A simple lightning parameterization for calculating global lightning distributions, J. Geophys. Res., 97, 9919–9933, 1992. 558

Rasch, P. J., Feichter, J., Law, K., et al.: A comparison of scavenging and deposition processes in global models: results from the WCRP Cambridge workshop of 1995, Tellus, , 52B, 1025–1056, 2000. 555

Restad, K., Isaksen, I. S. A., and Berntsen, T. K.: Global distributions of sulphate in the troposphere, a three-dimensional model study, Atmos. Environ., 32, 3593–3609, 1998.

Robertson, A., Overpeck, J., Rind, D., Mosley-Thompson, E., Zielinski, G., Lean, J., Koch, D., Penner, J., Tegen, I., and Healy, R.: Hypothesized climate forcing time series for the last 500 years, J. Geophys. Res., 106, 14783–14803, 2001. 554

Robock, A.: Volcanic eruptions and climate, Rev. Geophys., 38, 2, 191–219, 2000. 552

Robock, A. and Mao, J.: Winter warming from large volcanic eruptions, Geophys. Res. Lett., 19, 2405–2408, 1992. 553

Spiro, P. A., Jacob, D. J., and Logan, J. A.: Global inventory of sulfur emissions with 1∘ x 1∘ resolution, J. Geophys. Res., 97, 6023–6036, 1992. 558

Steingrímsson, J.: Fires of the Earth: the Laki eruption 1783–1784. Nordic Volcanological Institute and the University of Iceland Press, 1998. 553

Stevenson, D. S., Johnson, C. E., Collins, W. J., and Derwent, R. G.: Intercomparison and evaluation of atmospheric transport in a Lagrangian model (STOCHEM) and an Eulerian model (UM) using ^{222}Rn as a short-lived tracer, Q. J. R. Meteorol. Soc., 124, 2477–2491, 1998a. 555

Stevenson, D. S., Johnson, C. E., Collins, W. J., Derwent, R. G., Shine, K. P., and Edwards, J. M.: Evolution of tropospheric ozone radiative forcing, Geophys. Res. Lett., 25, 3819–3822, 1998b. 558, 559

Stevenson, D. S., Highwood, E. J., Johnson, C. E., Collins, W. J., Derwent, R. G.: Atmospheric modelling of the 1783–1784 Laki eruption, UGAMP Newsletter, 24, 43–44, 2001. 560

Stevenson, D. S., Johnson, C. E., Collins, W. J., and Derwent, R. G.: The tropospheric sulphur cycle and the role of volcanic SO_2, In: Volcanic degassing: Experiments, Models, Observations and Impacts,(eds. Oppenhiemer, C., D. Pyle, and J. Barclay), Geol. Soc. Spec. Pub., in press, 2003. 559

Stothers, R. B.: The great dry fog of 1783, Climatic Change, 32, 79–89, 1996. 554, 569, 586

Stothers, R. B.: Far reach of the tenth century Eldgjá eruption, Climatic Change, 39, 715–726, 1998. 571

Thordarson, T. and Self, S.: Sulfur, chlorine, and fluorine degassing and atmospheric loading by the Roza eruption, Columbia River Basalt group, Washington, USA, J. Volcanol. Geotherm. Res., 74, 49–73, 1996. 571

Thordarson, T. and Self, S.: Atmospheric and environmental effects of the 1783–1784 Laki eruption; a review and reassessment, J. Geophys. Res., 108, D1, 4011, doi:10.1029/2001JD002042, 2003. 553, 554, 561, 562, 569, 586

Thordarson, T., Self, S., Oskarsson, N., and Hulsebosch, T.: Sulfur, chlorine, and fluorine degassing and atmospheric loading by the 1783–1784 AD Laki (Skaftar Fires) eruption in Iceland, Bull. Volcanol., 58, 205–225, 1996. 553, 554, 561, 562, 569

Tie, X., Brasseur, G., Emmons, L., Horowitz, L., and Kinnison, D.: Effects of aerosols on tropospheric oxidants: A global model study, J. Geophys. Res., 106, 22931–22964, 2001. 569

Wallace, P. J.: Volcanic SO_2 emissions and the abundance and distribution of exsolved gas in magma bodies, J. Volcanol. Geotherm. Res., 108, 85–106, 2001. 561

Wang, Y. and Jacob, D. J.: Anthropogenic forcing on tropospheric ozone and OH since prein-

dustrial times, J. Geophys. Res., 103, 31123–31135, 1998. 558
Woods, A. W.: Moist convection and the injection of volcanic ash into the atmosphere, J. Geophys. Res., 98, 17627–17636, 1993. 561
Yienger, J. J. and Levy III, H.: An empirical model of global soil-biogenic NO_x emission, J. Geophys. Res., 100, 11447–11464, 1995. 558
Zielinski, G. A.: Stratospheric loading and optical depth estimates of explosive volcanism over the last 2100 years derived from the Greenland Ice Sheet Project 2 ice core, J. Geophys. Res., 100, 20937–20955, 1995. 554, 568, 569, 585, 586

Table 1. Sulphur chemistry: Gas- and aqueous-phase reactions, equilibria and Henry's Law coefficients. [M] is the molecular density of air (molecules cm^{-3}), $[H^+]$ is the hydrogen ion concentration (mol l^{-1}), T is temperature (K), $T^* = 1/T - 1/298$ (to be continued on next page)

Gas-phase reactions	Rate constants[a]
$SO_2 + OH + M \rightarrow H_2SO_4 + HO_2$	complex[e]: A6(A3)$^{(1/A7)}$
$DMS + OH \rightarrow CH_3SO + HCHO$	9.6×10^{-12} exp(-234/T)
$DMS + OH \rightarrow DMSO + HO_2$	complex[f]
$DMS + NO_3 \rightarrow CH_3SO + HCHO + HNO_3$	1.9×10^{-13}exp(520/T)
$CH_3SO + O_3 \rightarrow CH_3SO_2 + O_2$	6.0×10^{-13}
$CH_3SO + NO_2 \rightarrow CH_3SO_2 + NO$	8.0×10^{-12}
$CH_3SO_2 + O_3 \rightarrow CH_3SO_3 + O_2$	3.0×10^{-13}
$CH_3SO_2 + NO_2 \rightarrow CH_3SO_3 + NO$	4.0×10^{-12}
$CH_3SO_2 + O_2 \rightarrow CH_3O_2 + SO_2$	5.0×10^{13} exp(-(1.0+(8656/T)))
$CH_3SO_3 + HO_2 \rightarrow MSA$	5.0×10^{-11}
$CH_3SO_3 + O_2 \rightarrow CH_3O_2 + SA$	5.0×10^{13} exp(-(1.0+(11071/T)))
$CH_3SO_3 + HCHO \rightarrow MSA + CO + HO_2$	1.6×10^{-15}
$DMSO + OH \rightarrow DMSO_2 + HO_2$	5.8×10^{-11}
$DMSO_2 + OH \rightarrow CH_3SO_2CH_2O_2$	1.0×10^{-12}
$CH_3SO_2CH_2O_2 + NO \rightarrow NO_2 + HCHO + CH_3SO_2$	4.1×10^{-12} exp(180/T)
$CH_3SO_2CH_2O_2 + CH_3O_2 \rightarrow HO_2 + 2HCHO + CH_3SO_2$	3.0×10^{-13}
Species	**Henry's Law coefficients[b]**
SO_2	1.23×10^{0} exp(3120 T^*)
O_3	1.1×10^{-2} exp(2300 T^*)
HNO_3	3.3×10^{6} exp(8700 T^*)
H_2O_2	7.36×10^{4} exp(6621 T^*)
NH_3	7.5×10^{1} exp(3400 T^*)
CO_2	3.4×10^{-2} exp(2420 T^*)

Table 1. Continued

Aqueous-phase equilibria	Equilibrium constants[c]
$SO_2 + H_2O \rightleftharpoons H^+ + HSO_3^-$	1.7×10^{-2} exp(2090 T^*)
$HSO_3^- \rightleftharpoons H^+ + SO_3^{2-}$	6.0×10^{-8} exp(1120 T^*)
$HNO_3 \rightleftharpoons NO_3^- + H^+$	1.8×10^{-5} exp(-450.0 T^*)
$NH_3 + H_2O \rightleftharpoons NH_4^+ + OH^-$	1.8×10^{-5} exp(-450.0 T^*)
$CO_2 + H_2O \rightleftharpoons H^+ + HCO_3^-$	4.3×10^{-7} exp(-913.0 T^*)
$H_2O \rightleftharpoons H^+ + OH^-$	1.0×10^{-14} exp(-6716.0 T^*)
Aqueous-phase reactions	**Rate constants[d]**
$HSO_3^- + H_2O_2 \rightarrow H^+ + SO_4^{2-} + H_2O$	$([H^+]/([H^+]+0.1))\ 5.2\times10^6$ exp(-3650 T^*)
$HSO_3^- + O_3 \rightarrow H^+ + SO_4^{2-} + O_2$	4.2×10^5 exp(-4131 T^*)
$SO_3^{2-} + O_3 \rightarrow SO_4^{2-} + O_2$	1.5×10^9 exp(-996 T^*)

[a] Units $(cm^3\ molecule^{-1})^{(no.\ of\ reactants\ -\ 1)}\ s^{-1}$;
[b] Units $mol\ l^{-1}\ atm^{-1}$;
[c] Units $(mol\ l^{-1})^{(no.\ of\ products\ -\ no.\ of\ reactants)}$;
[d] Units $mol\ l^{-1}\ s^{-1}$;
[e] A1=[M]$3.0\times10^{-31}(T/300)^{-3.3}$; A2=$1.5\times10^{-12}$; A3=0.6; A4=0.75-1.27$\log_{10}$A3; A5=A1/A2; A6=A1/(1+A5); A7=1+$(\log_{10}A5/A4)^2$;
[f] $(1.7\times10^{-42}[O_2]\exp(7810/T))/(1+(5.5\times10^{-31}[O_2]\exp(7460/T)))$

Table 2. Emissions for the 1990 scenario. Units are $Tg\ yr^{-1}$, except SO_2 and DMS emissions which are $Tg(S)\ yr^{-1}$, and NO_x and NH_3 emissions which are $Tg(N)\ yr^{-1}$. "Other natural" includes 8.8 $Tg(S)\ yr^{-1}$ from background volcanic emissions, 5 $Tg(N)\ yr^{-1}$ from lightning, 69 $Tg(CH_4)\ yr^{-1}$ from tundra, 89 $Tg(CH_4)\ yr^{-1}$ from wetlands, and 27 $Tg(CH_4)\ yr^{-1}$ from termites. Anthropogenic NO_x includes 0.5 $Tg(N)\ yr^{-1}$ from aircraft

Species	Anthropogenic	Biomass burning	Vegetation	Soils	Oceans	Other natural
SO_2	71.2	1.4	–	–	–	8.8
DMS	–	–	–	1.0	15.0	–
NH_3	39.3	3.5	–	2.4	8.2	–
NO_x	23.3	7.1	–	5.6	–	5.0
CH_4	282.0	55.0	–	–	13.0	185.0
CO	393.0	500.0	150.0	–	50.0	–
H_2	20.0	20.0	–	5.0	5.0	–
C_2H_6	5.1	3.6	3.5	–	–	–
C_3H_8	5.3	1.0	3.5	–	0.5	–
C_4H_{10}	45.8	2.1	8.0	–	–	–
C_2H_4	5.8	7.1	20.0	–	–	–
C_3H_6	7.9	8.2	20.0	–	–	–
C_5H_8	–	–	450.0	–	–	–
C_7H_8	7.1	5.5	–	–	–	–
C_8H_{10}	7.2	1.1	–	–	–	–
HCHO	1.1	1.3	–	–	–	–
CH_3CHO	2.5	4.0	–	–	–	–
CH_3OH	6.0	7.5	–	–	–	–
CH_3COCH_3	2.1	0.5	20.0	–	–	–

Table 3. Sulphur dioxide and sulphate budgets. Fluxes have units of Tg(S), totalled over the year for the annual figures, and over June-July-August for the JJA figures (to be continued on next page)

	Annual				JJA			
	1990	1860	Laki Lo -1860	Laki Hi -1860	1990	1860	Laki Lo -1860	Laki Hi -1860
SO_2 sources								
SO_2 emissions	81.3	9.0	61.3	61.3	20.4	2.3	44.3	44.3
DMS → SO_2	11.7	12.2	0.0	0.0	3.0	3.1	0.0	0.0
SO_2 sinks								
SO_2 + OH	6.0	1.9	8.3	9.8	1.9	0.6	7.4	7.8
$HSO^-_{3(aq)}$ + $H_2O_{2(aq)}$	31.7	11.0	6.8	9.6	10.1	3.0	4.9	6.1
$HSO^-_{3(aq)}$ + $O_{3(aq)}$	0.2	0.1	0.1	0.1	0.0	0.0	0.1	0.1
$SO^{2-}_{3(aq)}$ + $O_{3(aq)}$	16.8	4.3	1.6	2.1	3.3	0.9	0.2	0.3
SO_2 dry deposition	28.9	1.8	21.0	17.1	6.7	0.4	15.2	12.3
SO_2 wet deposition	9.3	2.2	23.3	22.4	1.5	0.5	15.2	14.3
SO_2 burden (Tg(S))	0.29	0.09	1.51	2.67	0.18	0.07	4.36	6.60
SO_2 lifetime (days)	1.1	1.6	9.0	16.0	0.70	1.2	9.3	14.7

Table 3. Continued

	Annual				JJA			
	1990	1860	Laki Lo -1860	Laki Hi -1860	1990	1860	Laki Lo -1860	Laki Hi -1860
Sulphate sources								
SO_2 + OH	6.0	1.9	8.3	9.8	1.9	0.6	7.4	7.8
Aqueous phase SO_2 oxidation	48.8	15.4	8.5	11.7	13.4	3.9	5.1	6.5
DMS → H_2SO_4	0.3	0.1	0.0	0.0	0.1	0.0	0.0	0.0
Sulphate sinks								
H_2SO_4 dry deposition	2.6	0.7	2.0	2.1	0.9	0.2	1.5	1.4
H_2SO_4 wet deposition	21.4	9.7	14.7	19.2	6.1	2.5	10.3	11.6
$(NH_4)_2SO_4$ dry deposition	4.1	0.8	0.1	0.1	1.1	0.2	0.1	0.1
$(NH_4)_2SO_4$ wet deposition	27.0	6.1	0.1	0.2	7.1	1.6	0.1	0.1
H_2SO_4 burden (Tg(S))	0.40	0.19	0.30	0.54	0.51	0.20	0.91	1.14
$(NH_4)_2SO_4$ burden (Tg(S))	0.41	0.09	0.0	0.0	0.45	0.10	0.0	0.0
Total sulphate lifetime (days)	5.4	5.8	6.5	9.1	5.8	5.9	6.9	7.9

Table 4. Modelled and measured SO_4^{2-} depositions to Greenland Ice, for the Laki eruption, and background levels at the time of the eruption

	Background H_2SO_4 [mg(S) m^{-2} yr^{-1}]	Laki H_2SO_4 [mg(S) m^{-2}]
Modelled (this work)		
Laki Hi	5.0	63
Laki Lo	5.0	65
Measured		
Clausen and Hammer (1988) (Table IV)		
(H^+/ECM technique: 11 cores)	8.6±4.4	56±23
(SO_4^{2-} technique: 4 cores)	2.9±0.7	55±5
Zielinski (1995) (Table 6)		
GISP2 (SO_4^{2-} technique)	–	19
Clausen et al. (1997) (Table 3)		
DYE 3 (ECM technique)	7.9	33
GRIP (ECM technique)	4.3	23
Mosley-Thompson et al. (2002)		
PARCA cores: range from 6 cores	–	18-107

Table 5. Estimates of the total aerosol yield and peak global aerosol loading of the atmosphere from the Laki eruption

	Total aerosol yield [Tg(H_2SO_4)]	Peak aerosol loading [Tg(H_2SO_4)]
This work		
Laki Lo	51	4.4
Laki Hi	66	5.1
Clausen and Hammer (1988)	280	–
Zielinski (1995)	34-43	–
Stothers (1996)	150	4.5
Clausen et al. (1997)	101-153	–
Thordarson and Self (2003)	200	–

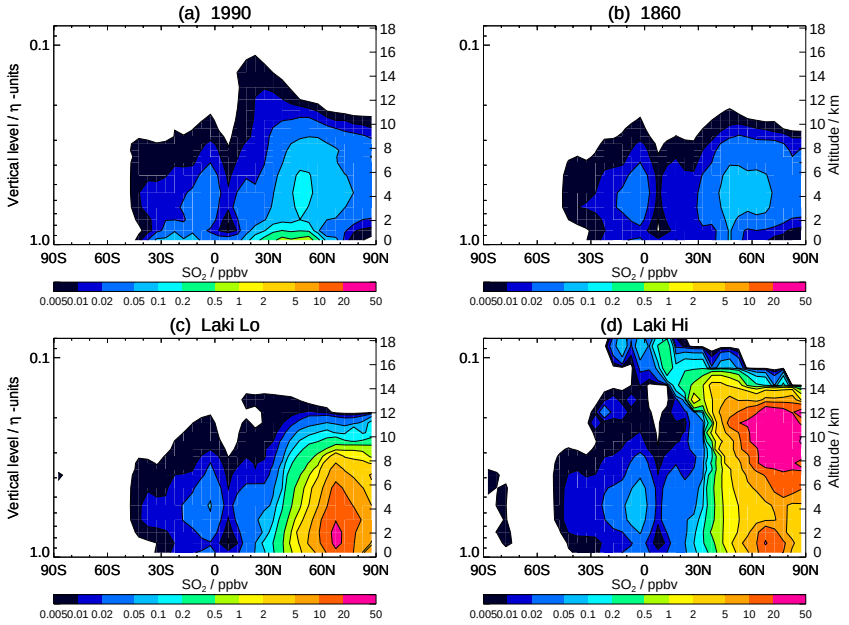

Fig. 1. Zonal, June-July-August (JJA) mean SO_2 concentrations (ppbv) for: **(a)** 1990; **(b)** 1860; **(c)** Laki Lo; and **(d)** Laki Hi.

587

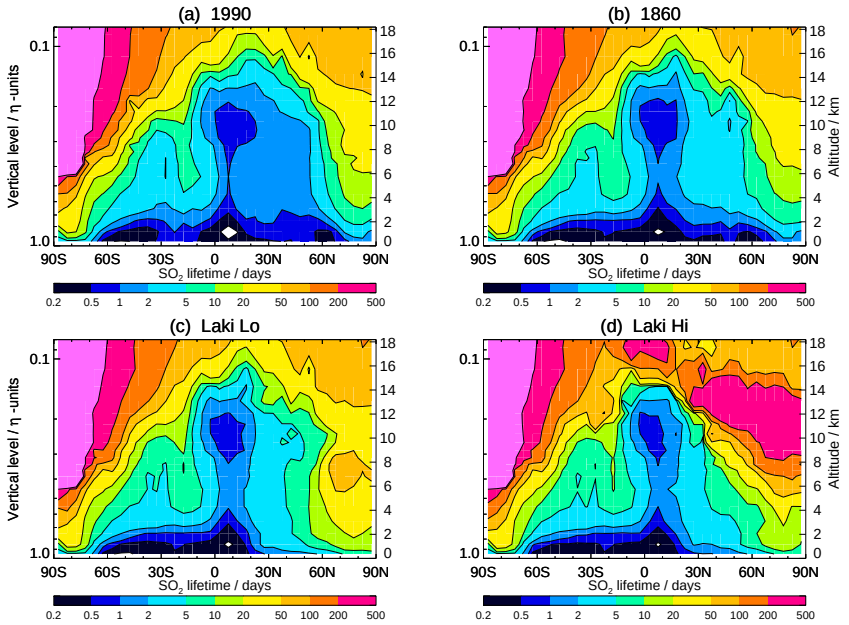

Fig. 2. Zonal, June-July-August (JJA) mean SO_2 lifetimes (days) for: **(a)** 1990; **(b)** 1860; **(c)** Laki Lo; and **(d)** Laki Hi.

588

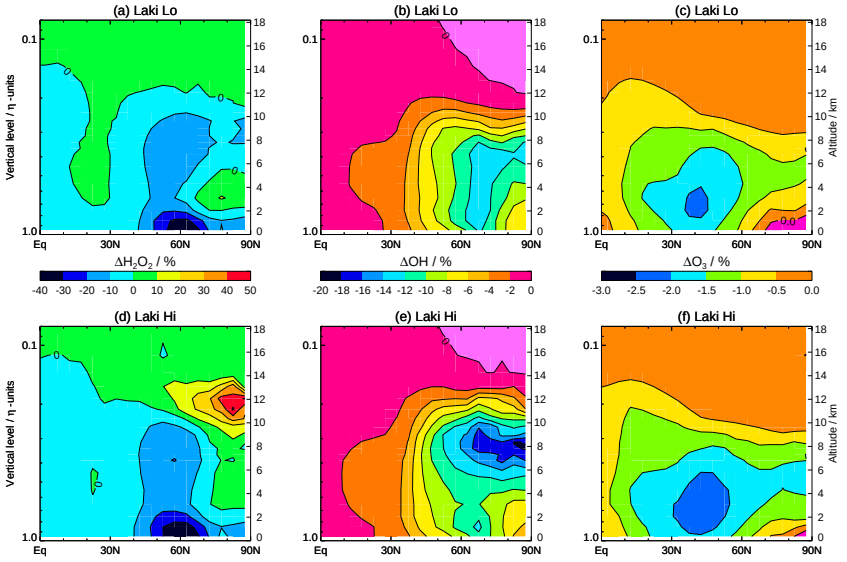

Fig. 3. Northern Hemisphere zonal, June-July-August (JJA) mean oxidant depletions (%) for Laki Lo **(a–c)** and Laki Hi **(d–f)**, relative to 1860. For each case, changes are plotted for: H_2O_2 (a, d); OH (b, e); and O_3 (c, f).

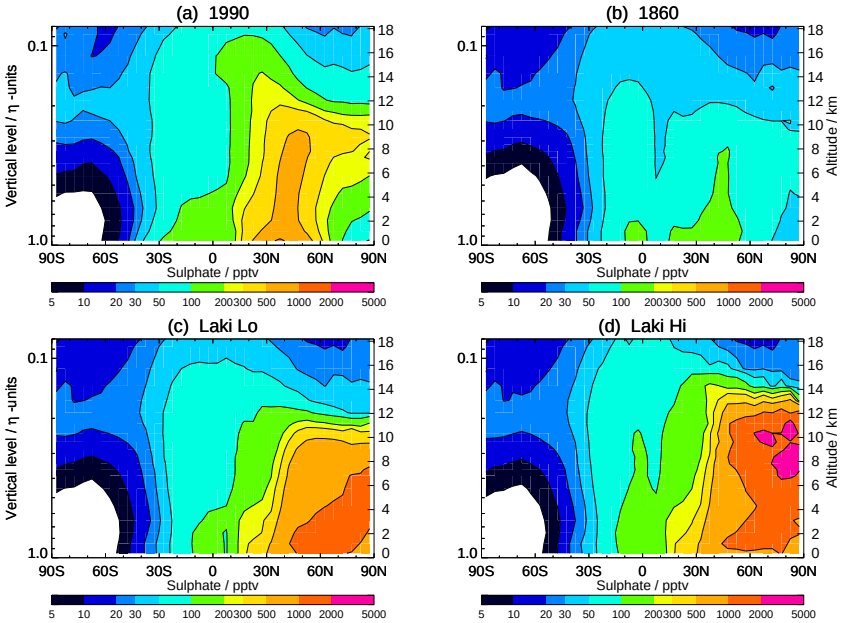

Fig. 4. Zonal, June-July-August (JJA) mean SO_4 concentrations (ppbv) for: **(a)** 1990; **(b)** 1860; **(c)** Laki Lo; and **(d)** Laki Hi.

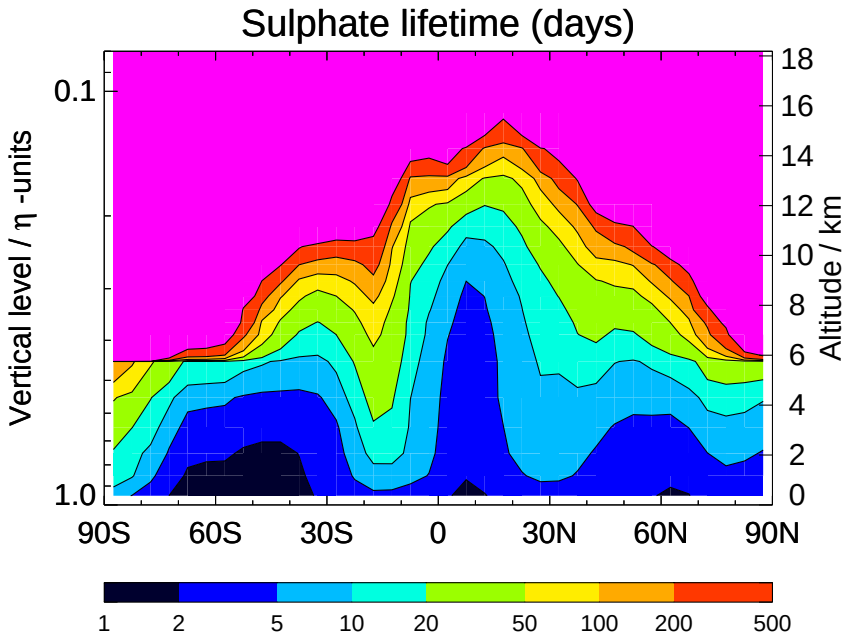

Fig. 5. Zonal, June-July-August (JJA) mean SO_4 lifetime (days) for the four scenarios (all scenarios are the same).

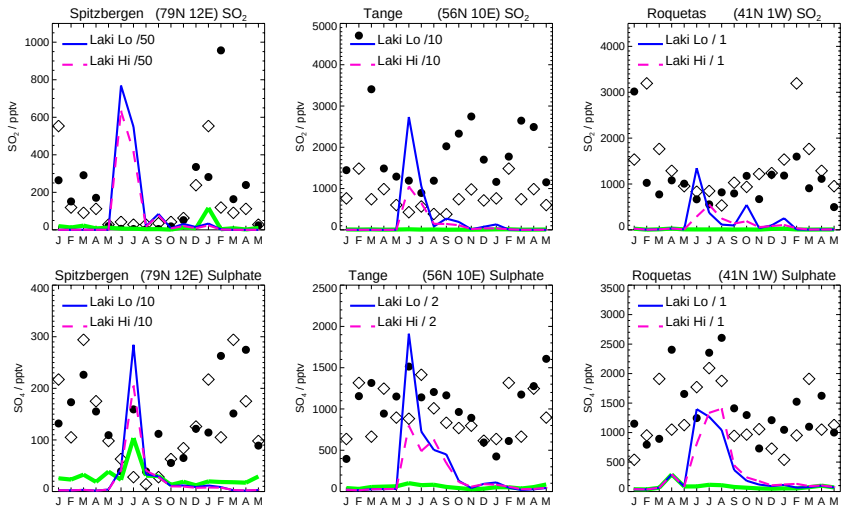

Fig. 6. Comparison of 1990 modelled SO_2 and SO_4 (•) with recent observations (⋄) (Hjellbrekke et al., 1996) at 3 European sites. The plot extends over 17 months of model results; observations are repeated for the second year. Also shown are results from the 1860 scenario (thick green line), and the two Laki scenarios (solid blue and dashed magenta lines), reduced by up to a factor of 50 to fit on the plots.

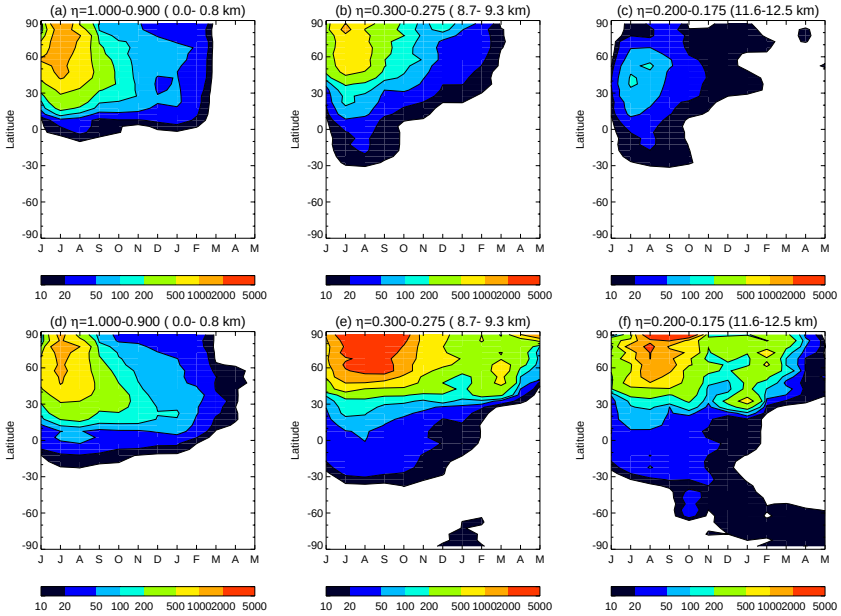

Fig. 7. Temporal evolution of the zonal mean Laki SO_4 (pptv) for Laki Lo **(a–c)** and Laki Hi **(d–f)**, at three levels in the model: the surface (a, d); the upper troposphere (b, e); and the lower stratosphere (c, f). Background 1860 levels have been subtracted.

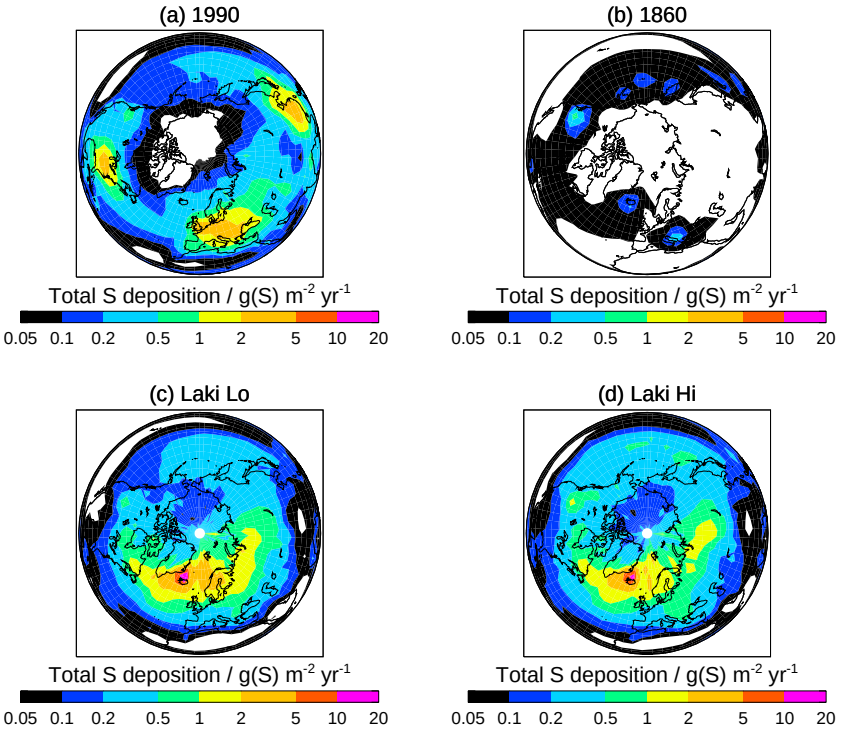

Fig. 8. Northern Hemisphere annual mean total sulphur deposition fluxes ($g(S)\,m^{-2}\,yr^{-1}$) for: **(a)** 1990; **(b)** 1860; **(c)** Laki Lo; and **(d)** Laki Hi.

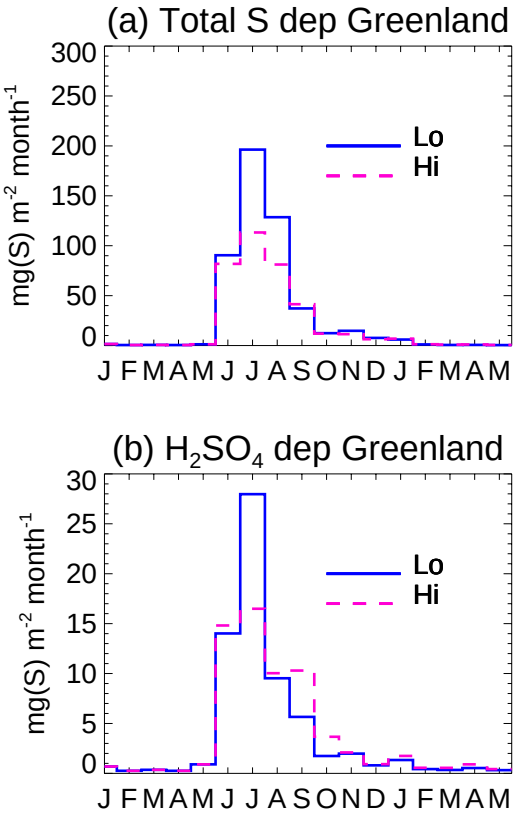

Fig. 9. Simulated monthly **(a)** total sulphur and **(b)** H_2SO_4 deposition fluxes (mg(S) m^{-2} $month^{-1}$) to central Greenland, for the two Laki scenarios.

595

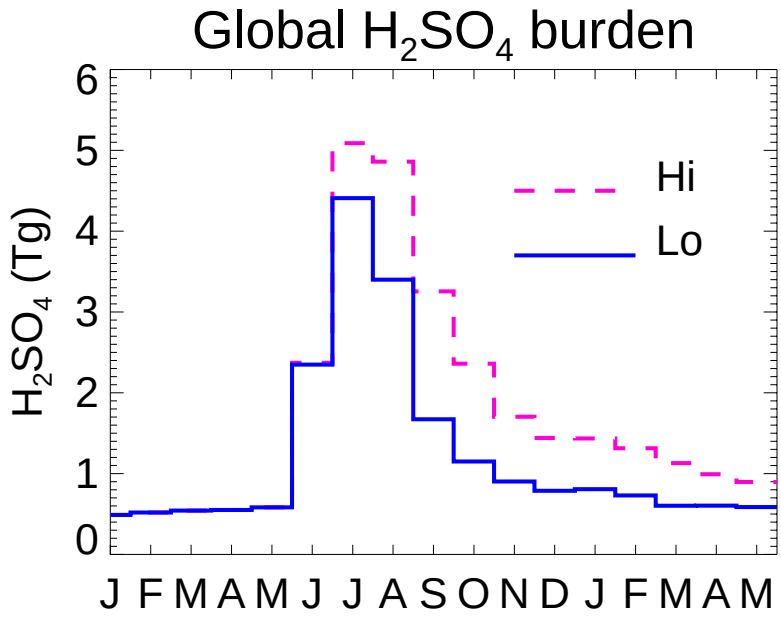

Fig. 10. Monthly global H_2SO_4 burden ($Tg(H_2SO_4)$), for the two Laki scenarios.

596